Aromaticity of Pyrene and Its Cyclopentafused Congeners—Resonance and NICS Criteria. An Ab Initio Valence Bond Analysis in Terms of Kekulé Resonance Structures

Remco W. A. Havenith,*,†,‡ Joop H. van Lenthe,*,† Fokke Dijkstra,† and Leonardus W. Jenneskens*,‡

Debye Institute, Theoretical Chemistry Group, Utrecht University, Padualaan 8, 3584 CH Utrecht, The Netherlands, and Debye Institute, Department of Physical Organic Chemistry, Utrecht University, Padualaan 8, 3584 CH Utrecht, The Netherlands

Received: September 18, 2000; In Final Form: December 13, 2000

The effect of cyclopentafusion on the aromatic properties of pyrene and its cyclopentafused congeners has been studied by calculating resonance energies, using the valence bond (VB) method, and nucleus independent chemical shifts using DIGLO. The VB resonance energy is only slightly affected by cyclopentafusion. The resonance interactions between Kekulé resonance structures that lead to six π electron (benzene-like) conjugated circuits have the largest contributions to the resonance energy, in favor of Clar's model. For all compounds these contributions are of similar magnitude. Hence, according to the resonance criterion, all compounds have the same aromatic character. In contrast, the total NICS values show a decrease of aromatic character of the compounds in the series upon the addition of externally fused five-membered rings. However, in line with the resonance criterion, the diamagnetic part of the shielding tensor perpendicular to the molecular framework is nearly constant for all compounds, provided that comparable gauge origins are chosen. Thus, care should be taken by comparing the aromatic character of rings of different molecules by considering only their total NICS values.

Introduction

Polycyclic aromatic hydrocarbons (PAHs) with external cyclopentafused five-membered rings, such as the cyclopentafused pyrene derivatives (Chart 1), belong to the class of nonalternant polycyclic aromatic hydrocarbons and may exhibit unusual (photo)physical properties, e.g. anomalous fluorescence and high electron affinities.[1,2]

Several qualitative models, e.g. Platt's ring perimeter model,[3] Clar's model,[4] and Randić's conjugated circuits model,[5−7] have either been or are frequently used for the rationalization of the properties and the reactivity of PAHs. According to Platt's ring perimeter model,[3] the aromatic hydrocarbon should be divided into two parts: a perimeter and an inner core. The perimeter should be considered as a [*n*]annulene, while the inner core represents only a perturbation. The properties of the hydrocarbon are then interpreted as those of the [*n*]annulene, using the Hückel $[4n + 2]$ rules.

Another view offers Clar's model[4] of aromatic hydrocarbons. In this model aromaticity is regarded as a local property. The Kekulé resonance structure with the largest number of aromatic sextets, i.e. benzene-like moieties, is preferred. The other rings in the PAH are less aromatic and are chemically more reactive.

The conjugated circuits model of Randić[5−7] takes both Clar's model and Platt's ring perimeter model into consideration. All distinct conjugated circuits, i.e. cyclic arrays of sp^2 hybridized carbon atoms, in all Kekulé resonance structures are considered with equal weight. This model is used for estimating the resonance energy of a PAH. All conjugated circuits have a contribution, depending on the number of π electrons. Those consisting of $[4n + 2]$ π electrons [$R(n)$] have a stabilizing (negative) contribution, while the [$4n$] conjugated circuits [$Q(n)$] have a destabilizing (positive) contribution. The parameters $R(n)$ and $Q(n)$ were chosen in order to reproduce the resonance energy[6] of small aromatic hydrocarbons obtained by using either valence bond (VB) calculations[8] or by comparing the total energies of the PAH with an appropriate polyene reference compound.[9] All these qualitative models rationalize the properties of aromatic and antiaromatic hydrocarbons in terms of the Hückel $[4n + 2]$ and [$4n$] rules.

The extra stability of a PAH, due to π electron delocalization, can also be determined, computationally or experimentally, by either considering homodesmotic relationships[10] or by the reaction enthalpy of the reaction of the PAH toward suitable chosen reference compounds.[11] For example, for pyrene (**1**) the isodesmic aromatic stabilization energy (ASE), which serves as a measure of the resonance energy, can be calculated as the energy difference between the methyl-substituted derivative and its quinoid derivative containing an *exo*-methylene substituent.

Other aromaticity criteria include the geometric criteria like the aromaticity indices I_5 and I_6 of Bird[12,13] and the harmonic oscillator model of aromaticity (HOMA).[14] Another approach to assess the aromatic properties of a PAH is by considering its magnetic properties. As a consequence of induced ring currents in their π systems,[15,16] the magnetic properties of aromatic compounds differ with respect to those of nonconjugated alkenes. Hence, magnetic properties[10] [large anisotropy of the magnetic susceptibility ($\Delta\chi$), exaltation of isotropic magnetic susceptibility (Λ), deshielded ring protons, and negative nucleus independent chemical shift (NICS) values[17]] are also frequently used as aromaticity criteria. The different aromaticity criteria are not univocal and the classical (geometric and energetic)

* Corresponding author. Tel.: +31 302534135. Fax.: +31 302537504. E-mail: remco@chem.uu.nl, joop@chem.uu.nl, jennesk@chem.uu.nl.
† Theoretical Chemistry Group.
‡ Department of Physical Organic Chemistry.

10.1021/jp003344k CCC: $20.00
Published on Web 03/22/2001

CHART 1: Structures of 1-7 and a Schematic Representation of Their Pyrene-type Kekulé Resonance Structures

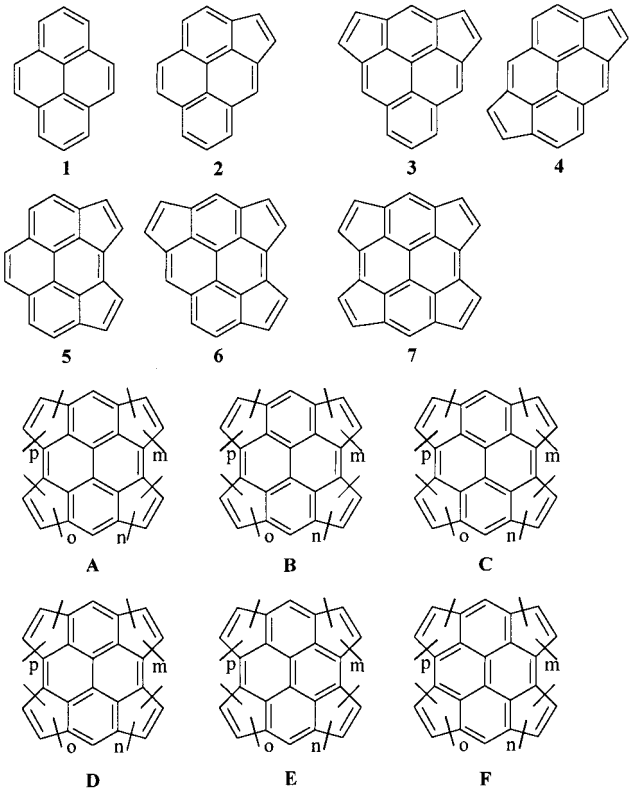

criteria are proposed to be orthogonal to the magnetic criteria.[18] However, the debate on the dimensionality of the concept of aromaticity is still ongoing.[10,19]

The anomalous magnetic properties and bond equalization result from cyclic electron delocalization, with which aromaticity is associated.[10] This cyclic electron delocalization results from resonance between two or more Kekulé resonance structures. A striking example is the structure of benzene, which cannot be described by one valence bond structure. Hückel theory and any other molecular orbital theory are one-determinant approaches and thus do not provide any information about the importance of the different structures. In contrast, VB theory can address the interaction between Kekulé resonance structures, since the wave function is written as a linear combination of these structures. Following the proposal by Pauling,[20] the resonance energy (E_{res}) of an aromatic hydrocarbon is calculated as the difference between the total VB energy and the energy of the most stable structure ($E_{res} = E_{tot} - E_{lowest}$). In addition, the weights of the different Kekulé resonance structures are accessible, which designate the importance of a particular structure in the wave function.

In a related study on the cyclopentafused pyrene congeners,[21] in which regular ab initio methods were used (RHF/6-31G* and B3LYP/6-31G*), we found that cyclopentafusion has a large effect on the magnetic properties of the congeners; a decrease of the aromatic character upon consecutive cyclopentafusion was found. The aromatic stabilization energies (ASEs) were unaffected, although the number of π electrons is increasing in this series. These effects prompted us to study the effect of cyclopentafusion in the cyclopentafused pyrene series on the interaction between the different Kekulé resonance structures and its effect on the resonance energy and thus its effect on their aromatic properties. VB theory enables us to partition the resonance energy into the contributions of the different conjugated circuits (vide infra). In this way, the aromatic properties of the individual rings can be studied using the resonance criterion and can be compared to the magnetic criteria for aromaticity. The results can be used for validating the fundamentals of the empirical models for describing PAHs.

Methods

Computational Details. All geometries of **1**−**7** were optimized using the GAMESS-UK[22] package at the RHF/6-31G level. Hessian calculations on **1**−**7** showed that planar **1**−**6** are real minima and that planar **7** possesses one imaginary frequency. The geometries obtained at the RHF/6-31G level of theory are in excellent agreement with those obtained at the RHF/6-31G* and B3LYP/6-31G* levels of theory.[21] In line are also the magnetic properties calculated at the RHF/6-31G, RHF/6-31G*, and B3LYP/6-31G* geometries, indicating that the RHF method using the 6-31G basis set gives an adequate description of the compounds. The equilibrium geometry of **7** was found to be bowl-shaped (vide infra).[21] This means that, in a treatment of the conjugated system in this geometry, σ orbitals cannot be excluded, as the strict σ/π separation is destroyed. The deviation from the planar form of **7** is rather small, as indicated by the angle of only 12.4° between the midpoint of the C(6)−C(8) bond, C(2) and C(6) (see Figure 1h). Previous VB studies of bent benzenes showed that the description of the π system does not change much for bending angles up to 50°.[23] Thus the VB results obtained for the planar transition state are expected not to deviate much from those of bowl-shaped **7**. In addition, the calculation on planar **7** is computationally much cheaper.

The VB calculations were performed with the TURTLE[24] program package. In the spirit of Pauling,[25] we considered only the Kekulé resonance structures (vide infra). The π system was described by strictly atomic, nonorthogonal p-orbitals, which were optimized for benzene (vide infra). The σ core was taken from a preceding RHF/6-31G calculation.

Nucleus independent chemical shift (NICS) values in the ring centers[17] were calculated using the Direct IGLO[16,26] program, at the RHF/6-31G geometry using the IGLO-III basis set. The chemical shift shielding tensor is given as a sum of the diamagnetic and paramagnetic part by the IGLO program.

Nomenclature of Valence Bond Structures. Before considering the possible valence bond structures for pyrene (**1**) and its cyclopentafused derivatives, the possibilities for benzene are presented. For benzene, five covalent structures are possible. Two of these are represented by the Kekulé resonance structures, in which the π bonds coincide with the σ bonds. Three other covalent structures exist, viz. the Dewarbenzene structures. In these structures, two of the three π bonds coincide with the σ bonds, while the third π bond connects the opposite site of the hexagon. The wave function of benzene is made up for more than 70% of the two Kekulé resonance structures.[23] Thus the three Dewarbenzene structures have only minor contributions.

For pyrene (**1**) 1430 covalent structures can be generated. Only six structures have all π bonds along the σ bonds. These six structures are the Kekulé resonance structures of pyrene. In the case of tetracyclopenta[*cd*,*fg*,*jk*,*mn*]pyrene (**7**), 208 012 covalent structures can be generated. Only ten Kekulé resonance structures exist for this molecule. It is expected that only the Kekulé resonance structures are important in the description of these molecules and that the other structures can be ignored.

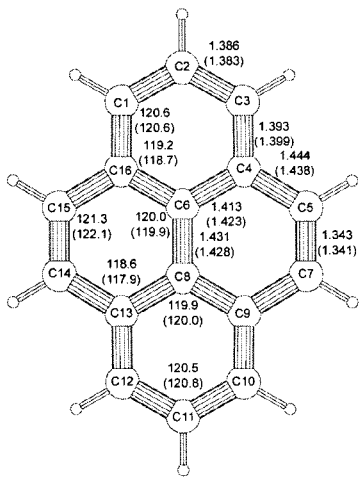

Figure 1a

1, D_{2h}

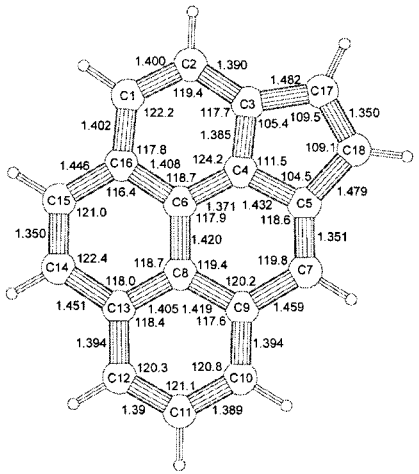

Figure 1b

2, C_s

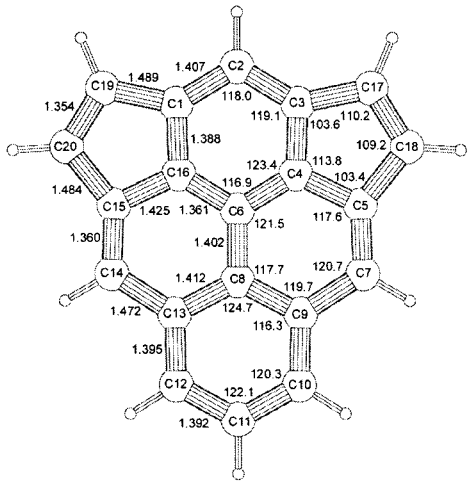

Figure 1c

3, C_{2v}

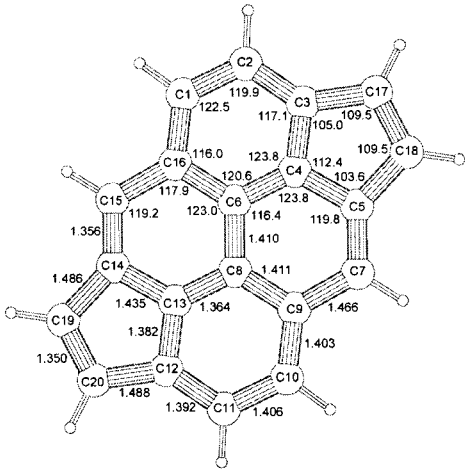

Figure 1d

4, C_{2h}

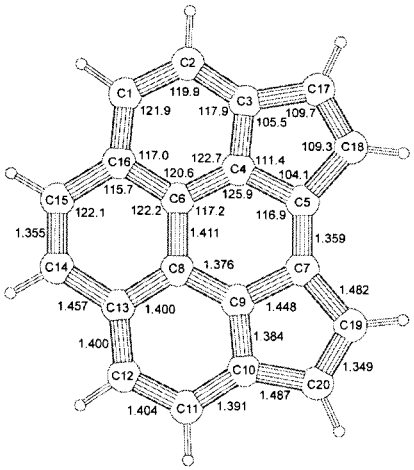

Figure 1e

5, C_{2v}

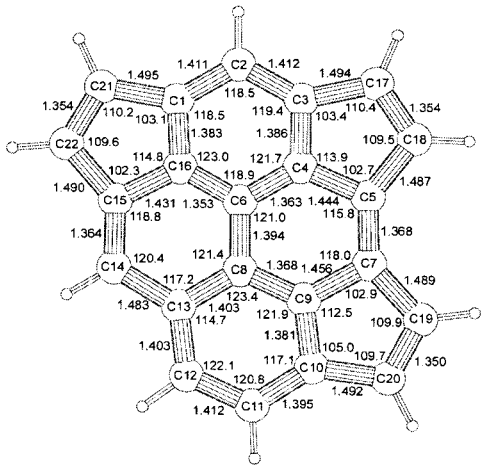

Figure 1f

6, C_s

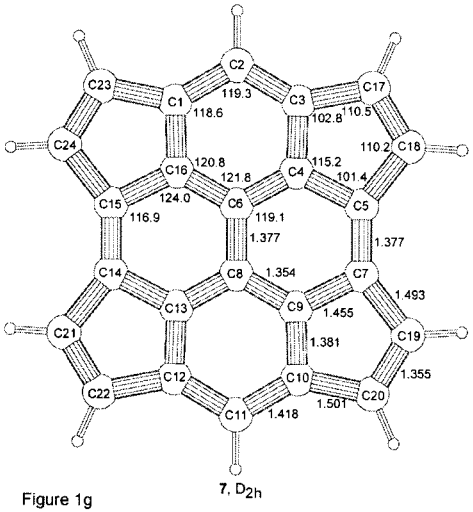

Figure 1g

7, D_{2h}

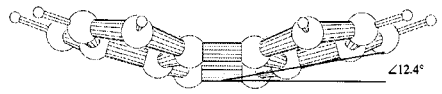

Figure 1h

Figure 1. Salient RHF/6-31G structural features of pyrene (**1**) (a) (experimental values in parentheses[28]), cyclopenta[*cd*]pyrene (**2**) (b), dicyclopenta[*cd,mn*]pyrene (**3**) (c), dicyclopenta[*cd,jk*]pyrene (**4**) (d), dicyclopenta[*cd,fg*]pyrene (**5**) (e), tricyclopenta[*cd,fg,jk*]pyrene (**6**) (f), planar tetracyclopenta[*cd,fg,jk,mn*]pyrene (**7**) (g) and side view of the equilibrium structure of tetracyclopenta[*cd,fg,jk,mn*]pyrene (h). Bond lengths are in Å and valence angles in degrees.

TABLE 1: Weights and Energies of the Kekulé Resonance Structures of 2 Calculated Using the Benzene Optimized p-Orbitals and the Optimized p-Orbitals for 2 (Chart 1)

	benzene-optimized p-orbitals		optimized p-orbitals for **2**	
structure	weight	E (au)	weight	E (au)
2A	0.216	−686.845 553	0.216	−686.845 623
2B	0.189	−686.837 622	0.189	−686.837 677
2C	0.193	−686.833 741	0.193	−686.833 809
2D	0.240	−686.847 528	0.240	−686.847 621
2E	0.083	−686.802 083	0.083	−686.802 107
2F	0.079	−686.802 020	0.079	−686.802 076
total E (a.u.)[a]	−686.940 798		−686.940 936	
E_{res} (kcal/mol)	−58.53		−58.56	

[a] RHF/6-31G total energy of **2**: −687.242053 au

Choice of the p-Orbitals. A VB calculation, in which the p-orbitals are optimized, is time-consuming. For example, in the case of cyclopenta[*cd*]pyrene (**2**), it takes 2 orders of magnitude more CPU time than a VB calculation with predetermined orbitals. The latter took 4 h of CPU time on a SGI-R10K. Therefore, all VB calculations were performed with predetermined (optimized for benzene) strictly atomic p-orbitals. To validate the applicability of these frozen p-orbitals, they were also optimized for **2**, viz. the smallest molecule in this series with low symmetry (C_s). The results show that the structure energies, their weights, and the resonance energy (E_{res}) are only marginally affected (Table 1).

Partitioning of the Resonance Energy. Besides an estimate of the total resonance energy ($E_{res} = E_{tot} - E_{lowest}$), which is a measure of the aromatic character of the compound,[20,25] the VB calculations also provide coefficients and interaction matrix elements of the individual resonance structures. This enables the identification of the most important resonance interactions between Kekulé resonance structures and in this way the most aromatic subsystems.

To analyze the individual contributions of different conjugated circuits to the resonance energy, the **H** matrix has to be transformed to an orthogonal basis. Thus, the structures are orthogonalized (Löwdin orthogonalization[27]) and the **H** matrix is transformed to this orthogonal basis, yielding $\mathbf{H}^{\perp}$. The total energy can then be partitioned in the weighted diagonal contributions of the structures ($\sum_i c_i^2 H_{ii}^{\perp}$) and the weighted resonance contributions between them ($c_i c_j H_{ij}^{\perp}$):

$$E = \sum_i \sum_j c_i c_j H_{ij}^{\perp} = \sum_i c_i c_i H_{ii}^{\perp} + \sum_i \sum_{j>1} 2 c_i c_j H_{ij}^{\perp} \quad (1)$$

where c_i is the coefficient of structure i in the wave function.

The sum of these resonance contributions is another measure of the resonance energy (E^{m}_{res}), namely, with respect to the weighted mean value of the energy of all structures. This mean resonance energy is thus more negative (stabilizing) than the Pauling resonance energy (E_{res}).[20] The E^{m}_{res} values for **1**−**7** follow the same trend as the E_{res} values (Table 3). This means that E^{m}_{res} can serve as a measure for the resonance energy E_{res}. The contribution to E^{m}_{res} of a particular interaction between two structures is 2 times the weighted resonance contribution ($2c_i c_j H_{ij}^{\perp}$). The differences between a pair of Kekulé resonance structures elucidate the conjugated circuit in which the π electrons are delocalized by resonance.

Results and Discussion

The RHF/6-31G Geometries of the Cyclopentafused Pyrene Derivatives. Whereas the optimized geometries of **1**−**6** were all found to be planar, that of **7** is bowl-shaped (Figure 1). The planar geometry of **7** is the transition state for bowl-to-bowl interconversion; an energy barrier of only 3.20 kcal/mol (for the RHF/6-31G level of theory; RHF/6-31G* gives 3.8 kcal/mol; B3LYP/6-31G* gives 2.9 kcal/mol[21]) is found.

TABLE 2: Weights of the Kekulé Resonance Structures of the Cyclopentafused Pyrene Derivatives and Their Relative Energy in Parentheses (in kcal/mol,[a] Chart 1)

compound	**A**	**B**	**C**	**D**	**E**	**F**
1 (D_{2h})	0.200	0.200	0.214	0.214	0.086	0.086
	(0.00)	(0.00)	(0.71)	(0.71)	(21.99)	(21.99)
2 (C_s)	0.216	0.189	0.193	0.240	0.083	0.079
	(1.24)	(6.22)	(8.65)	(0.00)	(28.52)	(28.56)
3 (C_{2v})	0.203	0.203	0.217	0.217	0.079	0.079
	(0.00)	(0.00)	(0.47)	(0.47)	(26.49)	(26.49)
4 (C_{2h})	0.203	0.203	0.176	0.267	0.075	0.075
	(7.81)	(7.81)	(16.62)	(0.00)	(36.52)	(36.52)
5 (C_{2v})	0.239	0.174	0.218	0.218	0.082	0.069
	(0.00)	(11.50)	(6.20)	(6.20)	(33.50)	(35.93)
6 (C_s)	0.223	0.189	0.243	0.198	0.076	0.068
	(0.75)	(6.52)	(0.00)	(7.90)	(34.26)	(36.23)
7 (D_{2h})[b]	0.208	0.208	0.222	0.222	0.068	0.068
	(0.00)	(0.00)	(0.13)	(0.13)	(35.19)	(35.19)

[a] Energy of the Kekulé resonance structure with the lowest energy: **1A/B**, −611.187290 au; **2D**, −686.847528 au; **3A/B**, −762.485737 au; **4D**, −762.505755 au; **5A**, −762.505340 au; **6C**, −838.142596 au; and **7A/B**, −913.774319 au. [b] Transition state for bowl-to-bowl interconversion.

In pyrene (**1**) a short C(5)−C(7) bond length of 1.343 Å (Figure 1a) is found. The bond lengths in the biphenyl-like substructure are all ca. 1.40 Å (range 1.413−1.386 Å), whereas the C(4)−C(5) bond length is substantially longer, viz. 1.444 Å. The RHF/6-31G geometry of **1** is in excellent agreement with that found by a single-crystal X-ray analysis at 93 K[28] (Figure 1a).

Cyclopentafusion has only a minor influence on the bond lengths of the pyrene substructure (see, for example, cyclopenta[*cd*]pyrene (**2**), Figure 1b). For all five-membered rings similar structural features are found, viz. typical single and double bond lengths between 1.479 and 1.501 Å and between 1.349 and 1.355 Å, respectively (Figures 1c−g). The C(4)−C(6) bond length of the pyrene substructure shortens significantly from 1.413 Å in **1** to 1.371 Å in **2** upon the introduction of a five-membered ring. In the other cyclopentafused pyrene congeners, the analogous carbon−carbon bond shortens equally upon cyclopentafusion (Figures 1a−g). Similarly, the introduction of a five-membered ring results in a slight decrease of the C(3)−C(4) bond length (~ -0.012 Å) and in a slight increase of the C(5)−C(7) bond length (~ 0.034 Å).

Valence Bond Description of Pyrene (1). The weights and relative energies of the Kekulé resonance structures **A**−**F** (Chart 1) of pyrene (**1**) are presented in Table 2. The larger weights of **A**−**D** compared to those of **E** and **F** indicate that **A**−**D** are more important in the VB description of **1**. The total resonance energy (E_{res}) of **1** equals −62.34 kcal/mol (Table 3), indicating a high degree of stabilization with respect to the most stable Kekulé resonance structure of **1**.

The partitioning of the resonance energy (Table 4) reveals a large contribution of −16.92 kcal/mol to the mean resonance energy (E^{m}_{res}) from the resonance interactions between **A**↔**C**, **A**↔**D**, **B**↔**C**, and **B**↔**D**. The resonance interaction between **A** and **C** (Chart 1) leads to a six π electron (benzene-like) conjugated circuit in the top six-membered ring of **1** (Chart 2). Electron delocalization within a six π electron conjugated circuit in the top and bottom six-membered rings is further a consequence of the resonance interaction between the structures

TABLE 3: Total Energies of Compounds 1-7 (in au) and Their Resonance Energies (in kcal/mol)

compound[a]	RHF	VB	E_{res}[b]	E^{m}_{res}[b]	E_{rel}[c]
1 (6)	−611.555 550	−611.286 631	−62.34	−100.90	
2 (6)	−687.242 053	−686.940 798	−58.53	−101.10	
3 (6)	−762.918 242	−762.584 880	−62.21	−101.77	4.70
4 (7)	−762.922 606	−762.592 661	−54.54	−101.49	1.96
4 (6)	−762.922 606	−762.592 523	−54.45	−101.32	
5 (7)	−762.925 727	−762.595 225	−56.40	−101.79	0.00
5 (6)	−762.925 727	−762.595 050	−56.29	−101.54	
6 (8)	−838.595 341	−838.236 025	−58.63	−102.68	
7 (10)	−914.259 921	−913.873 884	−62.48	−104.20	
7 (6)	−914.259 921	−913.873 345	−62.14	−103.44	

[a] The number of Kekulé resonance structures is indicated in parentheses. [b] For comparison, the resonance energies of benzene, calculated with localized p-orbitals (6-31G basis set) and two structures, are $E_{res} = -27.74$ kcal/mol and $E^{m}_{res} = -44.16$ kcal/mol. [c] Calculated at the RHF/6-31G level of theory, in kcal/mol relative to the energy of **5**.

TABLE 4: Contributions of the Interactions between the Orthogonalized Structures to the Resonance Energy (E^{m}_{res}) for Pyrene (1) in kcal/mol ($2c_ic_jH_{ij}^{\perp}$)

	A	**B**	**C**	**D**	**E**
B	−0.08				
C	−16.92	−16.92			
D	−16.92	−16.92	0.29		
E	−9.66	−0.18	−3.20	−3.20	
F	−0.18	−9.66	−3.20	−3.20	−0.96

CHART 2: Resonance between the Structures 1A and 1C, 1A and 1E, and 1A and 1F, Leading to Benzene-like Resonance in the Top Six π Electron, Central Six π Electron, and 14 π Electron Conjugated Circuits, Respectively

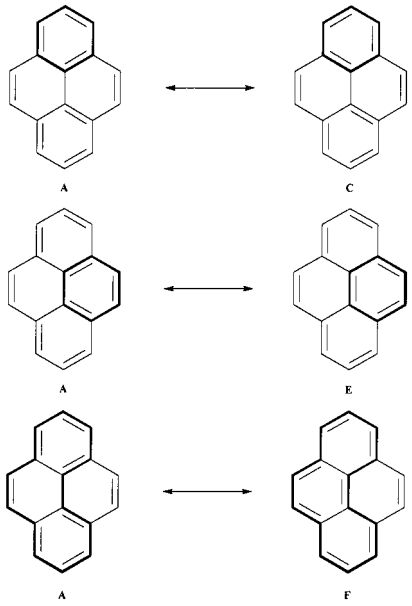

A↔D, **B↔C**, and **B↔D**. The interactions **A↔E** and **B↔F** (Charts 1 and 2) lead to a conjugated circuit in the right and left central six-membered ring, respectively, and have a contribution of −9.66 kcal/mol to E^{m}_{res}. The sum of all E^{m}_{res} contributions of the resonance interactions within the top and bottom six-membered rings is −67.68 kcal/mol (67.1%), while that of the central six-membered rings is −19.32 kcal/mol (19.1%). Other resonance interactions, e.g. **A↔F**, leading to a 14 π electron conjugated circuit (Charts 1 and 2), are responsible for the remaining part of E^{m}_{res} and contribute to a lesser extent (13.8%) to the total resonance energy.

The Effect of Cyclopentafusion. In a previous study, it was shown that the aromatic stabilization energies (ASEs) of the compounds **1**−**7** are all nearly equal,[21] i.e. cyclopentafusion has no effect on the resonance energy. This conclusion is confirmed by the VB calculations. The resonance energy (both E_{res} and E^{m}_{res}) of the compounds **1**−**7** are all of the same magnitude (Chart 1 and Table 3).

Upon the addition of externally fused five-membered rings, the weights and energies of the pyrene substructures are only marginally affected (Table 2). The structures with the lowest number of formal double bonds in the five-membered rings are energetically favored (Table 2 and Chart 1) and have the highest weights. The somewhat higher weights of the structures **2D**, **4D**, **5A**, and **6C** do not lead to a small degree of bond localization, since cyclopentafusion only affects the C(4)−C(6) type bonds significantly.

The contributions of the different conjugated circuits to E^{m}_{res} show for all compounds the same trends; the six π electron (benzene-like) conjugated circuits in the top and bottom six-membered rings (**A↔C**, **B↔D**, **A↔D**, **B↔C**) have the highest contribution to E^{m}_{res}, independent of cyclopentafusion.

The interactions between two Kekulé resonance structures with the lowest number of double bonds within the five-membered rings have the largest contribution to E^{m}_{res}. For example, for **2**, both the interactions **A↔D** and **B↔C** lead to benzene-like resonance in the bottom six-membered ring. The structures **A** and **D** have both one double bond in the five-membered ring, while the structures **B** and **C** have two double bonds (Chart 1). The structures **A** and **D** have therefore a lower energy compared to structures **B** and **C** (Table 2), and consequently their contribution to E^{m}_{res} is larger (Table 5). The same reasoning also rationalizes the differences between the contribution to E^{m}_{res} of the resonance interactions within the central six-membered rings (Table 5 and Chart 1). Thus, the small differences in the contributions of similar conjugated circuits to E^{m}_{res} in the series can be related to the energy differences between the Kekulé resonance structures.

The partitioning of the mean resonance energy (E^{m}_{res}) of **6** and **7** into contributions from different conjugated circuits is similar to that of **2** and **1**, respectively (Table 5). The benzene-like resonances in the top and bottom six-membered rings have the highest contribution to the mean resonance energy. The different contributions of the same-sized conjugated circuits are again related to the energy differences between the Kekulé resonance structures (Tables 2 and 5).

In addition to the six pyrene substructures, compounds **4**−**7** possess the Kekulé resonance structures depicted in Chart 3. However, their contribution to E^{m}_{res} is only small; they have negligible weights. Further support for the marginal influence of these resonance structures on E_{res} and E^{m}_{res} comes from VB calculations performed for **4**, **5**, and **7** with only the inclusion of the pyrene substructures. A decrease of E_{res} of only ca. 0.4 kcal/mol is observed (Table 3) and the structure weights are unaffected. Hence, all compounds should be seen as substituted pyrene derivatives.

Resonance Energy (E_{res}) as a Measure of Stability? The relative energy of the isomers **3**−**5** and their resonance energy are presented in Table 3. As noted previously,[21] the relative stability order of **5** > **4** > **3** does not follow the trend in the order of the resonance energy (E_{res}) of **3** > **5** > **4**.

A comparison of the energies of the most stable Kekulé resonance structures (Chart 1 and Table 2) of **3**−**5** shows that the energy of the most stable structure of **3** (**A**/**B**) is 12.3 kcal/mol higher than that of **5** (**A**). The energy difference between

TABLE 5: Contributions of the Interactions between the Orthogonalized Structures to the Resonance Energy (E^{m}_{res}) for Cyclopenta[*cd*]pyrene (2), Dicyclopenta[*cd,mn*]pyrene (3), Dicyclopenta[*cd,jk*]pyrene (4), Dicyclopenta[*cd,fg*]pyrene (5), Tricyclopenta[*cd,fg,jk*]pyrene (6), and Tetracyclopenta[*cd,fg,jk,mn*]pyrene (7) in kcal/mol ($2c_ic_jH_{ij}^{\perp}$)

Cyclopenta[*cd*]pyrene (**2**)

	A	B	C	D	E
B	−0.09				
C	−16.82	−15.68			
D	−18.32	−17.54	0.30		
E	−10.05	−0.18	−2.99	−3.37	
F	−0.19	−9.04	−2.93	−3.27	−0.87

Dicyclopenta[*cd,mn*]pyrene (**3**)

	A	B	C	D	E
B	−0.09				
C	−17.54	−17.00			
D	−17.00	−17.54	0.30		
E	−9.61	−0.19	−3.11	−3.14	
F	−0.19	−9.61	−3.14	−3.11	−0.81

Dicyclopenta[*cd,jk*]pyrene (**4**)

	A	B	C	D	E	F
B	−0.08					
C	−15.65	−15.65				
D	−19.01	−19.01	0.31			
E	−9.32	−0.18	−2.71	−3.39		
F	−0.18	−9.32	−2.71	−3.39	−0.77	
G	−0.08	−0.08	−0.04	−0.13	−0.03	−0.03

Dicyclopenta[*cd,fg*]pyrene (**5**)

	A	B	C	D	E	F
B	−0.09					
C	−18.58	−16.17				
D	−18.58	−16.17	0.31			
E	−10.63	−0.18	−3.16	−3.16		
F	−0.14	−8.13	−2.89	−2.89	−0.78	
G	−0.16	−0.03	−0.09	−0.09	0.01	−0.17

Tricyclopenta[*cd,fg,jk*]pyrene (**6**)

	A	B	C	D	E	F	G
B	**−0.08**						
C	−19.25	−17.58					
D	−17.19	−16.33	0.32				
E	−9.98	−0.18	−3.24	−2.92			
F	−0.14	−8.67	−3.08	−2.76	−0.71		
G	−0.15	−0.03	−0.10	−0.08	0.01	−0.17	
H	−0.09	−0.08	−0.12	−0.04	−0.03	−0.03	0.02

Tetracyclopenta[*cd,fg,jk,mn*]pyrene (**7**)

	A	B	C	D	E	F	G	H	I
B	−0.08								
C	−17.89	−17.89							
D	−17.89	−17.89	0.35						
E	−9.26	−0.14	−2.94	−2.94					
F	−0.14	−9.26	−2.94	−2.94	−0.64				
G	−0.08	−0.08	−0.05	−0.11	−0.03	−0.03			
H	−0.08	−0.08	−0.11	−0.05	−0.03	−0.03	0.00		
I	−0.03	−0.14	−0.09	−0.09	−0.17	0.01	0.02	0.02	
J	−0.14	−0.03	−0.09	−0.09	0.01	−0.17	0.02	0.02	0.00

4D and **5A** is only −0.26 kcal/mol. Since **3**−**5** contain the same number of π electrons, the significant energy difference between **3A/B** and **5A** has to originate from the σ skeleton.

The strain energy for these isomers has been deduced from homodesmotic reactions and distorted cyclopenta[*cd*]pyrene isomers, fixed in a geometry to match those of **3**−**5**.[21] The strain energy of **3** is 5.2 kcal/mol higher than that of **5**.

CHART 3: Remaining Kekulé Resonance Structures of 4, 5, 6, and 7 with Their Weights and Their Relative Energies (in kcal/mol)

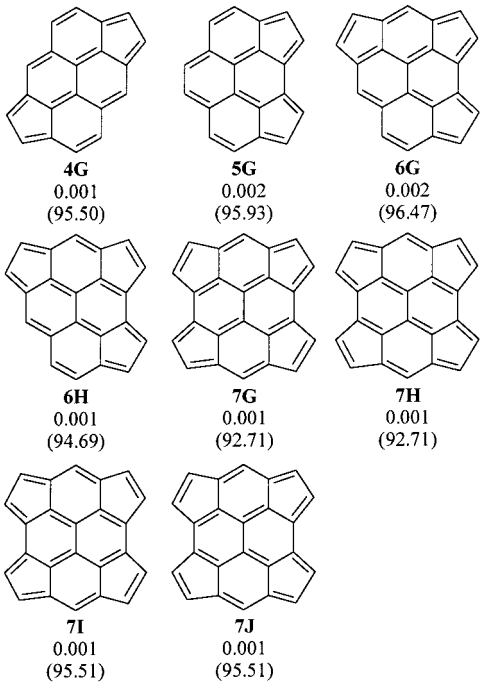

CHART 4: NICS Values of Compounds 1-7 at the Ring Centers

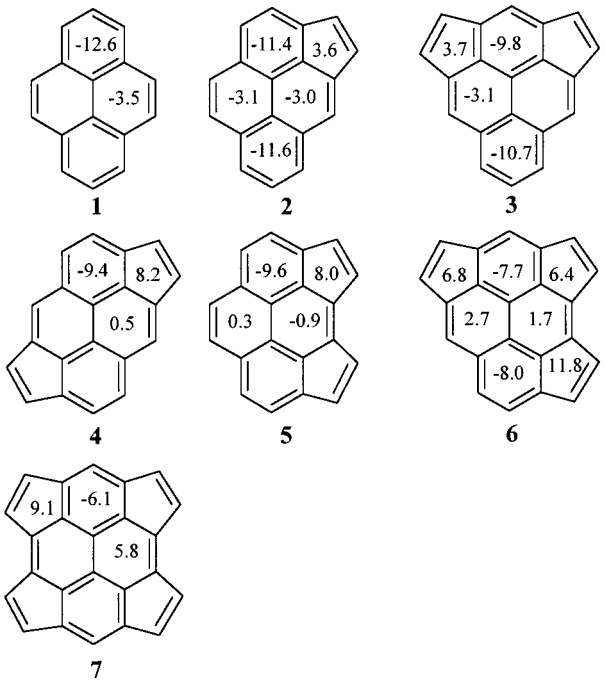

Thus, the relative stability of the dicyclopentafused-pyrene isomers cannot be deduced from a consideration of the resonance energy alone (cf. ref 21 and Subramanian et al.[29]).

Magnetic Properties versus the Valence Bond Results. Magnetic properties of polycyclic aromatic compounds are frequently used as aromaticity criteria.[10,17] The NICS values calculated at the ring centers for the compounds **1**−**7** are depicted in Chart 4. Large negative NICS values are found for the top and bottom six-membered rings. The NICS values for these rings are shifted 10 ppm upfield with respect to the NICS

CHART 5: Diamagnetic Part of the Shielding Tensor Perpendicular to the Molecular Plane ($NICS^d_\perp$) of the NICS Values of Compounds 1-7 Calculated at the Ring Centers[a]

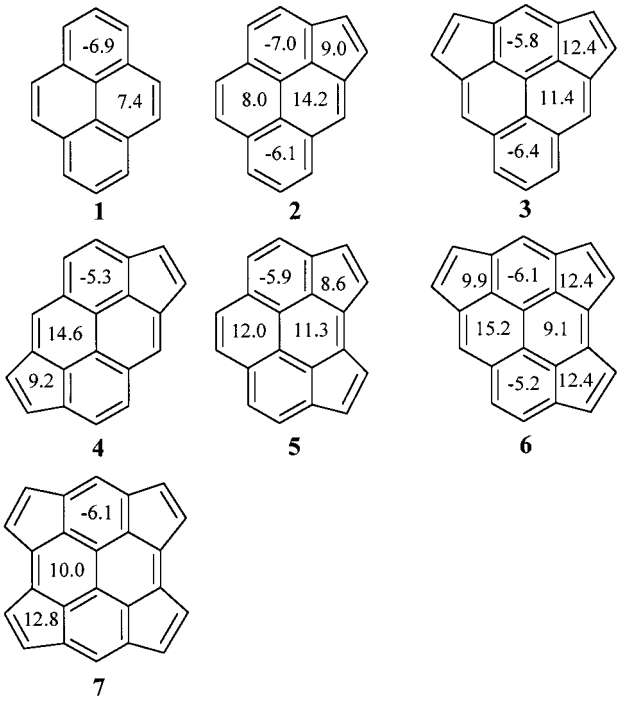

[a] The gauge origins of the localized MOs are chosen as the charge centroids of all drawn bonds. A single line denotes a LMO in the plane of the molecule and a double line denotes two banana bonds, one above and one below the plane of the molecule.

values of the central six-membered rings, which is in line with the resonance criterion, derived above.

Upon the addition of externally fused five-membered rings, the NICS values at the ring centers suggest a reduction of the aromatic character in this series. The resonance criterion (both E_{res} and E^m_{res}), however, does not suggest that the aromatic character of **1**−**7** decreases. To resolve this apparent discrepancy, one should consider the origin of the NICS criterion. Kutzelnigg et al.[16] showed that in the case of D_{6h} benzene, the paramagnetic contribution to the out-of-plane component of the magnetic susceptibility due to the π electrons vanishes, if the gauge origin is chosen in the ring center. This concept was extended and referred to as the nucleus independent chemical shift (NICS).[17] The diamagnetic contribution of the chemical shielding tensor perpendicular to the molecular framework ($NICS^d_\perp$) is indicative for the induced ring currents. For benzene, the NICS and the $NICS^d_\perp$ are equal. Unfortunately, for systems that do not possess this high symmetry, the paramagnetic contribution does not vanish and $NICS^d_\perp$ may deviate from the total NICS value. To get an estimate of the induced ring current when applying an external magnetic field, the $NICS^d_\perp$ values should be considered. In addition, for a meaningful comparison of different $NICS^d_\perp$ values, the gauge origins should be comparable, as the diamagnetic and paramagnetic contributions are gauge dependent, while the total shielding is not. As a result of the gauge dependence, the meaning of absolute $NICS^d_\perp$ values has disappeared, and the $NICS^d_\perp$ values can only be used for comparing the aromatic character of similar rings of different molecules.

The IGLO procedure requires localized molecular orbitals (LMOs). These LMOs are indicated by *all* drawn bonds in Chart 5. The employed localization procedure allows σ/π mixing, resulting in banana bonds for double bonds. The gauge origins in our IGLO calculations are chosen as the charge centroids of these LMOs. Several subgroups with comparable gauge origins can be identified. The gauge origins for the top and bottom six-membered rings are evenly distributed. The values of the $NICS^d_\perp$ of these six-membered rings are of equal magnitude (Chart 5), in line with the resonance criterion. The gauge origins are not comparable for the central six-membered rings and the five-membered rings, as the number of endo-cyclic double bonds, of which the charge centroids are chosen as the gauge origins, is not the same for all rings. The central six-membered rings can be divided into three subgroups and the five-membered rings into two, according to the number of endo-cyclic double bonds. The first subgroup of the central six-membered rings is composed by the right ring of **1**, the left ring of **2**, the right ring of **6**, and the left ring of **7**, all containing three endo-cyclic double bonds. The subgroup of two endo-cyclic double bonds contains the right ring of **3** and both central rings of **5**. The last subgroup of one endo-cyclic double bond consists of the right ring of **2** and the left rings of **4** and **6**. In a similar way, the five-membered rings of **2**, **4**, and **5** and the left ring of **6** can be grouped together and those of **3** and **7** and the right rings of **6**. The $NICS^d_\perp$ values of the rings within each subgroup have comparable magnitudes (Chart 5). From this point of view, the magnetic criteria also suggest that cyclopentafusion does not affect the aromatic character of the pyrene skeleton, in line with E_{res} and E^m_{res}.

It can therefore be concluded that the diamagnetic part of the chemical shielding tensor of the NICS values perpendicular to the molecular framework is indicative for resonance in a particular ring, but for comparing these values, equivalent gauge origins should be ensured. Hence, a comparison of total NICS values should be cautiously applied.

The Valence Bond Results in Relation to the Empirical Models. Since the contributions to the resonance energy for electron delocalization around the ring perimeter are negligible, no support for Platt's ring perimeter model[3] is found. For example, the contribution to E^m_{res} from resonance between the structures **5A** and **5G** (Charts 1 and 3) is only −0.16 kcal/mol (Table 5).

The VB calculations show that the Kekulé resonance structures with the maximum number of aromatic sextets have the lowest energy. The resonance interactions in these sextets have the largest contribution to the resonance energy, in line with Clar's model.[4]

The resonance energies obtained for this series using the conjugated circuits model are not in agreement with those obtained from the VB calculations (Table 6). The differences in resonance energy of these compounds are a consequence of the existence of [4*n*] π electron conjugated circuits, according to the conjugated circuits model. In contrast, the VB calculations show that for all compounds only the pyrene substructures are important. Thus the assumption of equal importance of all conjugated circuits leads to substantial errors in the derived resonance energy.

Conclusions

VB calculations with the inclusion of all Kekulé resonance structures on the cyclopentafused pyrene derivatives show that cyclopentafusion has only a modest effect on their resonance energies (both E_{res} and E^m_{res}), in line with their aromatic stabilization energies (ASEs). Only small differences in weights of the pyrene substructures are found. The six π electron (benzene-like) conjugated circuits have the largest contribution

TABLE 6: Resonance Energy of the Compounds 1-7 as Estimated Using Randić's Conjugated Circuits Model[5−7] in kcal/mol

compd	resonance energy[a]	reson energy
1	[12*R*(1)+8*R*(2)+6*R*(3)]/6	−49.95
2	[12*R*(1)+8*R*(2)+6*R*(3)]/6	−49.95
3	[12*R*(1)+8*R*(2)+6*R*(3)]/6	−49.95
4	[12*R*(1)+8*R*(2)+6*R*(3)+12*Q*(4)]/7	−40.45
5	[12*R*(1)+8*R*(2)+6*R*(3)+2*Q*(3)+8*Q*(4)+2*Q*(5)]/7	−40.24
6	[12*R*(1)+8*R*(2)+6*R*(3)+4*Q*(3)+20*Q*(4)+2*Q*(5)]/8	−32.28
7	[12*R*(1)+8*R*(2)+6*R*(3)+12*Q*(3)+28*Q*(4)+4*Q*(5)]/10	−21.95

[a] $R(n)$ and $Q(n)$ represent $[4n + 2]$, with $n = 1, 3$, and $[4n]$, with $n = 1, 5$, π-electron conjugated circuits, respectively. The E_{res} values of $R(n)$ and $Q(n)$ were taken from ref 6. Stabilization is denoted by a negative contribution to the resonance energy; $R(1) = -20.04$ kcal/mol, $R(2) = -5.67$ kcal/mol; $R(3) = -2.31$ kcal/mol; $Q(1) = 36.90$ kcal/mol; $Q(2) = 10.38$ kcal/mol; $Q(3) = 3.46$ kcal/mol and $Q(4) = 1.38$ kcal/mol. $Q(5)$ is assumed to be 0.00 kcal/mol.

to the resonance energy. The contributions to the resonance energy of these six π electron conjugated circuits are of nearly equal magnitude within this series. Cyclopentafusion only affects the energies of the pyrene substructures. Kekulé resonance structures in which the five-membered rings participate in π electron delocalization are unimportant, in line with Clar's model of aromatic hydrocarbons.

Care should be taken in comparing the aromatic character of rings of different molecules by considering the total NICS values. The diamagnetic part of the shielding tensor perpendicular to the molecular framework is nearly constant throughout the series, provided that similar gauge origins are chosen.

References and Notes

(1) For example: Gooijer, C.; Kozin, I.; Velthorst, N. H.; Sarobe, M.; Jenneskens, L. W.; Vlietstra, E. J. *Spectrochim. Acta Part A* **1998**, *54*, 1443−1449 and references cited.

(2) Sarobe, M. Ph.D. thesis *Polycyclic Aromatic Hydrocarbons under High-Temperature Conditions. Consequences for Carbon Build Up during Combustion and Fullerene Formation Processes*; Utrecht University: Utrecht, The Netherlands, 1998.

(3) Platt, J. R. *J. Chem. Phys.* **1954**, *22*, 1448−1455.

(4) Clar, E. *Polycyclic Hydrocarbons*; Academic Press Inc.: London, 1964.

(5) Randić, M. *Chem. Phys. Lett.* **1976**, *38*, 68−70.

(6) Randić, M. *Tetrahedron* **1977**, *33*, 1905−1920.

(7) Randić, M. *J. Am. Chem. Soc.* **1977**, *99*, 444−450.

(8) Herndon, W. C.; Ellzey, M. L. J. *J. Am. Chem. Soc.* **1974**, *96*, 6631−6642.

(9) Dewar, M. J. S.; de Llano, C. *J. Am. Chem. Soc*. **1969**, *91*, 789−795.

(10) A review of different aromaticity criteria: von R. Schleyer, P.; Jiao, H. *Pure Appl. Chem.* **1996**, *68*, 209−218.

(11) Mo, Y.; Jiao, H.; Lin, Z.; von R. Schleyer, P. *Chem. Phys. Lett.* **1998**, *289*, 383−390.

(12) Bird, C. W. *Tetrahedron* **1985**, *41*, 1409−1414.

(13) Bird, C. W. *Tetrahedron* **1986**, *42*, 89−92.

(14) For a review: Krygowski, T. M.; Cyrañski, M. K.; Czarnocki, Z.; Häfelinger, G.; Katritzky, A. R. *Tetrahedron* **2000**, *56*, 1783−1796.

(15) Pauling, L. *J. Chem. Phys.* **1936**, *4*, 673−677.

(16) Fleischer, U.; Kutzelnigg, W.; Lazzeretti, P.; Mühlenkamp, V. *J. Am. Chem. Soc.* **1994**, *116*, 5298−5306.

(17) von R. Schleyer, P.; Maerker, C.; Dransfeld, A.; Jiao, H.; van Eikema Hommes, N. J. R. *J. Am. Chem. Soc*. **1996**, *118*, 6317−6318.

(18) Katritzky, A. R.; Karelson, M.; Sild, S.; Krygowski, T. M.; Jug, K. *J. Org. Chem.* **1998**, *63*, 5228−5231.

(19) Bird, C. W. *Tetrahedron* **1996**, *52*, 9945−9952.

(20) Pauling, L.; Wheland, G. W. *J. Chem. Phys.* **1933**, *1*, 362−374.

(21) Havenith, R. W. A.; Jiao, H.; Jenneskens, L. W.; van Lenthe, J. H.; Sarobe, M.; von R. Schleyer, P.; Kataoka, M.; Necula, A.; Scott, L. T. To be submitted.

(22) Guest, M. F.; van Lenthe, J. H.; Kendrick, J.; Schöffel, K.; Sherwood, P.; Harrison, R. J., *GAMESS-UK, a package of ab initio programs*, 2000. With contributions from Amos, R. D.; Buenker, R. J.; Dupuis, M.; Handy, N. C.; Hillier, I. H.; Knowles, P. J.; Bonacic-Koutecky, V.; von Niessen, W.; Saunders: V. R. and Stone, A. J. It is derived from the original GAMESS code due to Dupuis, M.; Spangler, D. and Wendolowski, J., *NRCC Software Catalog, Vol. 1*, Program No. QG01 (GAMESS) 1980.

(23) Dijkstra, F.; van Lenthe, J. H. *Int. J. Quantum Chem.* **1999**, *74*, 213−221.

(24) Verbeek, J.; Langenberg, J. H.; Byrman, C. P.; Dijkstra, F.; van Lenthe, J. H., *TURTLE, an ab initio VB/VBSCF program*, 1988−2000.

(25) Pauling, L. *The Nature of the Chemical Bond and the Structure of Molecules and Crystals: An Introduction to Modern Structural Chemistry*., 3rd ed.; Cornell University Press: Ithaca, NY, 1960.

(26) Meier, U.; van Wüllen, C.; Schindler, M. *J. Comput. Chem.* **1992**, *13*, 551−559.

(27) Löwdin, P. O. *Rev. Mod. Phys.* **1967**, *39*, 259−287.

(28) Frampton, C. S.; Knight, K. S.; Shankland, N.; Shankland, K. *J. Mol. Struct.* **2000**, *520*, 29−32.

(29) Subramanian, G.; von R. Schleyer, P.; Jiao, H. *Angew. Chem., Int. Ed. Engl.* **1996**, *35*, 2638−2641; Subramanian, G.; von R. Schleyer, P.; Jiao, H. *Angew. Chem.* **1996**, *108*, 2824−2827.